HHS Public Access

Author manuscript

*Dev Biol*. Author manuscript; available in PMC 2021 June 15.

Published in final edited form as:

*Dev Biol*. 2020 June 15; 462(2): 119–128. doi:10.1016/j.ydbio.2020.02.016.

# Optic vesicle morphogenesis requires primary cilia

**Luciano Fiore**[#a], **Nozomu Takata**[#a], **Sandra Acosta**[a,b], **Wanshu Ma**[a], **Tanushree Pandit**[c], **Michael Oxendine**[a], **Guillermo Oliver**[a,*]

[a]Center for Vascular and Developmental Biology, Feinberg Cardiovascular and Renal Research Institute (FCVRRI), Northwestern University, Chicago, IL, USA

[b]Institute of Evolutive Biology, Pompeu Fabra University, Barcelona, Spain

[c]Department of Genetics, St. Jude Children's Research Hospital, Memphis, TN, USA

[#] These authors contributed equally to this work.

## Abstract

*Arl13b* is a gene known to regulate ciliogenesis. Functional alterations in this gene's activity have been associated with Joubert syndrome. We found that in *Arl13* null mouse embryos the orientation of the optic cup is inverted, such that the lens is abnormally surrounded by an inverted optic cup whose retina pigmented epithelium is oddly facing the surface ectoderm. Loss of *Arl13b* leads to the disruption of optic vesicle's patterning and expansion of ventral fates. We show that this phenotype is consequence of miss-regulation of Sonic hedgehog (*Shh*) signaling and demonstrate that the $Arl13b^{-/-}$ eye phenotype can be rescued by deletion of *Gli2,* a downstream effector of the *Shh* pathway. This work identified an unexpected role of primary cilia during the morphogenetic movements required for the formation of the eye.

### Keywords

Eye; Mouse; Shh; Morphogenesis; Arl13b; Primary cilia; Optic vesicle

## 1. Introduction

The primary cilia is a hair-like organelle present in the surface of most vertebrate cells (Berbari, O'Connor, Haycraft and Yoder, 2009). It is responsible for receiving and processing chemical and mechanical cues from the multicellular environment, including light from photoreceptor cells (Wheway et al., 2014), mechanical forces (Malone et al., 2007; Nishimura et al., 2019) and growth factors (Nishimura et al., 2019). Because of the diversity of interactors that each primary cilia can establish, their functional roles diverge

[*]Corresponding author. guillermo.oliver@northwestern.edu (G. Oliver).

Author contributions

L.F., N.T., and G.O. designed the experiments and analyzed the data. L.F., N.T., MO, WM and S.A. performed most of the experiments. L.F., NT and G.O. wrote the manuscript.

Declaration of competing interest

The authors declare no competing interests.

Appendix A. Supplementary data

Supplementary data to this article can be found online at https://doi.org/10.1016/j.ydbio.2020.02.016.

from cell to cell depending on the precise environment at a particular moment (Wallingford and Mitchell, 2011). This functional variability is central for developmental processes, as it was first demonstrated in genetic experiments showing that cilia are required for viability and patterning of the mouse embryo (Huangfu et al., 2003). Cilia defects can also affect many signaling pathways and cilia deficiencies underlie several neural abnormalities in humans (D'Angelo and Franco, 2009; Ware et al., 2011).

Joubert Syndrome (JS) is a rare ciliopathy that mainly affects the brain. JS is divided into six main clinical subgroups; one subgroup is JS with ocular defects (JS-O) (Makino and Tampo, 2014; Valente et al., 2008; Valente et al., 2013). This subgroup has been associated with mutations in *Arl13b* (JBTS8) (Cantagrel et al., 2008; Thomas et al., 2014; Valente et al., 2013), an ADP-ribosylation factor within the Ras superfamily of regulatory GTPases abundant in cilia and required for ciliogenesis in multiple organs (Caspary et al., 2007). *Arl13b*$^{-/-}$ mice exhibit the hennin (Hnn) phenotype, characterized by defects in cilia structure resembling those described in JS (Caspary et al., 2007; Thomas et al., 2014). In this particular murine model, cilia are present but are shorter than in wild type and are functionally impaired (Caspary et al., 2007; Larkins et al., 2011). It has been reported that *Arl13b*$^{-/-}$ mouse embryos have abnormal eyes (Caspary et al., 2007). It was also recently shown that conditional deletion of *Arl13b* in the mouse retina during later developmental stages is essential for retinogenesis and outer segment morphogenesis (Dilan et al., 2019). However, no detailed characterization of possible functional roles of *Arl13b*$^{-/-}$ during early stages of the eye morphogenesis has yet been reported.

In mice, the first morphological evidence of optic vesicle development is their symmetrical bilateral evagination from the diencephalon at around embryonic (E) day 8.0 (Adler and Canto-Soler, 2007; Heavner and Pevny, 2012). Each optic vesicle grows outward, such that it will eventually contact the lens placode within the surface ectoderm, thereby inducing lens formation (Ashery-Padan et al., 2000). At E10.5, the optic vesicles become a two-layer optic cup with the inner layer forming the neural retina (NR) and the outer layer forming the retinal pigment epithelium (RPE) which connects to the diencephalon via the optic stalk (OS) (Adler and Canto-Soler, 2007; Yun et al., 2009). The optic-vesicles (OVs) opening face toward the surface ectoderm; as development proceeds the lens is located inside the optic cup's aperture.

Optic vesicle morphogenesis is dependent on multiple signals, including *Shh* originating from the ventral midline, *FGFs* and *BMPs* from the presumptive lens ectoderm, and *TGF-ß* superfamily ligands from the cephalic mesenchyme (Bharti et al., 2006; Chow and Lang, 2001; Martinez-Morales et al., 2004; Yun et al., 2009). An interesting link between cilia and *Shh* signaling has been provided by data showing that in many cases, defects resulting from alterations in embryonic cilia are consequence of defective *Shh* signal transduction (Caspary et al., 2007; Endoh-Yamagami et al., 2009; Houde et al., 2006; Huangfu and Anderson, 2005; Vierkotten et al., 2007). Previous studies have also shown that primary cilia act mainly as regulators of the cell cycle and of the *Shh* and *Wnt* signaling pathways (D'Angelo and Franco, 2009).

To gain a better understanding on the functional role of cilia during early eye morphogenesis we took advantage of *Arl13b*$^{-/-}$ standard and conditional mouse strains. We found that in *Arl13b*$^{-/-}$ embryos the morphogenesis of the OVs is defective, such that the lens is abnormally surrounded by an inverted optic cup whose RPE is oddly facing the surface ectoderm. Using *Six3*$^{Cre}$ *and Wnt1*$^{Cre}$ to conditionally delete *Arl13b* we determined that this particular phenotype is consequence of *Arl13b* deletion in the neural tissue. Furthermore, we also determined that this phenotype is the result of *Shh* signaling miss-regulation leading to abnormal dorsal-ventral identity. Finally, we show that the *Arl13b*$^{-/-}$ eye phenotype is rescued by deletion of the downstream effector of the *Shh* pathway *Gli2*.

## 2. Results

### 2.1. Defective eye development in Arl13b mutant mice

*Arl13b*$^{-/-}$ embryos and heterozygous littermates were analyzed at E11.5 and E12.5 (Fig. 1 A-B'; phenotype is fully penetrant and representative figures are shown along the manuscript). *Arl13b*$^{-/-}$ embryos exhibit excencephaly, with flaps of neural tissue extending over the side of the head (n = 31 embryos, 16 litters). Initial morphological analysis showed that all *Arl13b*$^{-/-}$ embryos have bilateral defective eyes in which only the RPE was evident (Fig. 1A', B′ white arrows indicate the defective eyes). Detailed molecular characterization of the eye revealed a very intriguing phenotype. As seen in coronal sections of the mouse head in Fig. 1C-H' (all sections are at the same level as the optic stalk), the orientation of the optic-cups and their surrounding RPE appears inverted in *Arl13b*$^{-/-}$ embryos, such that the optic-cups opening was abnormally facing toward the inside of the diencephalic stalk, instead than toward the surface ectoderm. Furthermore, at this stage the β-crystallin-expressing lens was abnormally engulfed by the Rax-expressing optic cups blocking their normal contact with the surface ectoderm (Fig. 1C'). Although the mutant optic-cups are inverted, they expressed the typical NR and RPE markers at this stage, such as Vsx2 and Mitf (Fig. 1D, D').

To evaluate possible NR patterning defects, we performed immunostainings against Vax2, a marker for the ventral retina (Barbieri et al., 2002). As shown in Fig. 1E, Vax2 expression is restricted to the ventral retina of E12.5 *Arl13b*$^{+/-}$ optic vesicles. Conversely, in *Arl13b*$^{-/-}$ embryos Vax2 expression is expanded all throughout the NR (Fig. 1E'); a result suggesting that the mutant NR is abnormally ventralized. Interestingly, the lens is also not properly oriented. As shown in Fig. 1F', the orientation of the Pdgfrα-positive germinal epithelium and the developing Prox1-positve lens fibers also appears to be abnormal in the mutant eye, such that the lens fibers are elongating toward the opposite direction that in their normal littermate controls. Additionally, the lens fibers appear shorter and reduced in number when compared to those in *Arl13b*$^{+/-}$ littermates (Fig. 1F). Basal laminin deposition highlighted the morphological inversion of the eye, and shows that the basal polarity of the eye is normal in the mutant embryos (Fig. 1G').

At around E12.5, the ciliary marginal zone (CMZ) is normally detected in the peripheral-most region of the retina, in the interphase with the RPE (Belanger et al., 2017).To better understand the anatomy of the mutant eyes, we evaluated the expression of Otx2, a marker for the RPE and CMZ. As shown in Fig. 1H (green arrows), the presumptive CMZ is

restricted to the interphase between the retina and the RPE in E12.5 *Arl13b*$^{+/-}$ embryos. Conversely, in *Arl13b*$^{-/-}$ embryos the CMZ appears to be missing, as indicated by the lack of Otx2 expression along the optic-cup territory (Fig. 1H'). As expected, the optic fissure at the optic stalk level is completely closed in *Arl13b*$^{+/-}$ embryos (Fig. 1H white arrow indicates the optic nerve); instead the optic fissure is still open in mutant littermates (Fig. 1H' white arrow and Fig. 2A,B). We also found that expression of the optic stalk marker Pax2 was abnormally expanded into the region of the outer optic cup in *Arl13b*$^{-/-}$ embryos (Fig. 2C', C″), suggesting that the proximal-distal axis of the optic cup is not properly established in the mutant eye. Furthermore, we also found that expression of the dorsal optic cup marker Tbx5 is missing in the *Arl13b*$^{-/-}$ optic cup (Fig. 2D-E″), a result suggesting that dorsal-ventral patterning is also affected in these mutant optic cups.

These initial results argue that the *Arl13b* mutant optic cups and lens are abnormally inverted, such that the ventral optic cup appears to overgrowth and engulf the developing lens (Fig. 7A',B' and 6, 7, 8); however, the molecular identity of the main eye tissues (RPE, lens and NR) appears normal, although the NR appears to be ventralized and the CMZ is not properly established (Fig. 1I, I').

### 2.2. Molecular characterization of the Arl13b$^{-/-}$ optic vesicles

To better understand how loss of *Arl13b* function impacts eye development we examined earlier stages of eye morphogenesis. At E9.5, the OVs normally evaginate toward the overlying Six3 and Pax6 positive surface ectoderm (lens placode) that later on will give rise to the lens (Fig. 3A-D). Instead, the mutant OVs exhibit an abnormal shape, likely consequence of their unusual bending toward the ventral side of the diencephalon (Fig. 3A'-D′). In addition to these obvious morphological alterations, we also analyzed the expression of different molecular markers required during eye development. Six3 is normally expressed in the OVs, lens placode and ventral diencephalon (Fig. 3A) (O. Lagutin et al., 2001; Liu et al., 2010; Oliver et al., 1995). In *Arl13b* $^{-/-}$ embryos the Six3-expressing domains in the lens placode and OVs are narrower, and its level of expression in those two tissues also appears reduced (Fig. 3A' white arrow). In contrast, its expression level in the ventral diencephalon appears to be increased (Fig. 3A' green arrow). Similar alterations were observed with the OV and lens placode marker Pax6 (Fig. 3B) (Ashery-Padan et al., 2000; Liu et al., 2006), whose expression was also narrower and reduced in the mutant OVs and lens placode (Fig. 3B'). In control embryos, expression of one of the Bmp pathway (dorsal promoting signal) target genes, Lhx2, is detected throughout the entire OV and surrounding neural tissues (Fig. 3C) (Horner and Caspary, 2011; Yun et al., 2009); instead, its expression was drastically reduced in *Arl13b* $^{-/-}$ OVs (Fig. 3C'); a result that is in agreement with the absence of Tbx5 (dorsal marker) expression shown in Fig. 2. The pan-neural marker Sox1 is not expressed in the distal OVs of control embryos (Fig. 3D) (Wood and Episkopou, 1999); however, we found that it is ectopically expanded into the distal portion of the evaginating mutant OVs (Fig. 3D'). These results demonstrated that *Arl13b* activity is required for the normal formation and patterning of the developing mammalian OVs and lens placode.

Next, we aimed to determine which of the Arlb13-expressing tissue types were responsible for the eye phenotype. We took advantage of an *Arlb13* conditional mouse strain (Su et al.,

2012) that we crossed with *Cre* lines expressed in neural crest (*Wnt1*$^{Cre;}$ neural crest eventually migrates to the ocular mesenchymal region) and forebrain (*Six3*$^{Cre}$). No obvious eye phenotype was observed when using *Wnt1*$^{Cre}$ (Fig. 4A'); however, conditional null *Arl13b* embryos generated using *Six3*$^{Cre}$ exhibited an inverted OV phenotype similar to the one seen in standard *Arl13b*$^{-/-}$ null embryos (Fig. 4A''). This suggests that cilia defects in the diencephalon are likely responsible for the mutant phenotype.

### 2.3. Arl13b deficiency impacts the Shh pathway

Next, we aimed to identify the molecular mechanisms responsible for the observed eye phenotype. *Shh* signaling from the ventral midline is necessary for axial patterning, as during dorso-ventral patterning Shh establishes ventral identity in the OVs (Take-uchi, Clarke and Wilson, 2003). The identified alterations in dorsal-ventral patterning, as well as the expanded expression of the ventral NR marker Vax2 and the optic stalk marker Pax2 suggested that defects in the *Shh* pathway could be responsible for the phenotype (Perron et al., 2003). Furthermore, it is known that Shh drives expression of the ventralizing transcription factors Vax1 and Vax2, as overexpression of Shh expands Vax gene expression into the dorsal OVs; instead, Vax induction fails in the absence of *Shh* signaling (Mui et al., 2005; Take-uchi et al., 2003). It is known that *Shh* signaling distribution is mediated by primary cilia components, and Caspary et al. (2007) showed that in *Arl13b* mutant embryos this signal is defective (Caspary et al., 2007). Accordingly, whole-mount in situ hybridization of E9.5 mutant embryos showed that *Shh* expression was reduced in the ventral diencephalon, but it was ectopically expanded into the dorsal portion (Fig. 5A'; white arrow indicates dorsal and green arrow ventral diencephalon). Next, we evaluated the expression of the *Shh* pathway effector *Gli1* (Burnett et al., 2017). Whole-mount in situ hybridization of E9.5 mutant embryos showed that *Gli1* expression is ectopically expressed in the dorsal diencephalon, including the anterior forebrain (Fig. 5B, B′ white arrow indicates dorsal diencephalon). The ectopic expression of Shh was validated by immunostaining (Fig. 5C' white arrows indicate dorsal and green arrow ventral diencephalon). Importantly, in agreement with these results, expression of Nkx2.1, a downstream target of *Shh* signaling, was ectopically expressed into the mutant dorsal diencephalon (Fig. 5D' white arrow). This result suggested that in the mutant embryos the dorsal diencephalon acquired a ventral identity.

Previous ectopic expression studies demonstrated that Shh has a mitogenic role during central nervous system development (Belgacem et al., 2016; Rowitch et al., 1999). To analyze if at least some of the morphological defects identified in the mutant OVs were a consequence of abnormal proliferation, we performed immunostainings against Ki67. We found that in the mutant OVs proliferation was increased from 4.32% to 12.65% (Suppl Fig. 1A-A′). However, we did not find significant differences in cell death around the optic vesicle using a TUNEL assay at this stage (Suppl Fig. 1B-B′).

These results indicated that during OV morphogenesis, Arl13b activity in neural cilia is essential for modulating Shh signaling along the dorsal-ventral axis and thus, is necessary for establishing proper dorso-ventral polarity of the OVs. Some of those morphogenetic roles could be mediated by its regulation of OV proliferation.

### 2.4. Arl13b restricts the Shh pathway within the eye

The ectopic Shh expression and the upregulation of *Gli1* detected in the dorsal diencephalon of *Arl13b* null embryos (Fig. 5A'-C′) suggested that Arl13b is required to restrict *Shh* activity. To test this hypothesis, we took advantage of a $Gli2^{Lacz/+}$ mouse strain. Gli2 is the primary transcriptional activator for *Shh* signaling in the neural tube (Lebel et al., 2007) and *Gli2* knockout embryos are not excencephalic and their eyes are normal (Bai and Joyner, 2001; Mo et al., 1997). Accordingly, we generated *Arl13b;Gli2* double mutant mice to test whether loss of Gli2 could rescue the *Arl13b* null phenotype. As shown in Fig. 6, we found that the eye phenotype was rescued in E11.5 $Arl13b^{-/-};Gli2^{Lacz/+}$ embryos (Fig. 6A, A′). Immunostaining against the neural retina marker Rax and the lens marker β-crystallin revealed that the orientation of the neural retina and lens in $Arl13b^{-/-};Gli2^{Lacz/+}$ mutant embryos was rescued in these mutant embryos (Fig. 6B, B′). Arl13b immunostaining was used to confirm the Arl13b mutant phenotype (Fig. 6C, C′). Thus, we concluded that Arl13b restricts the *Shh* pathway within the eye field.

These results indicated that during OV morphogenesis, *Arl13b* activity in neural cilia is essential to modulate *Shh* signaling along the dorsal-ventral axis and therefore, to establish DV polarity of the OVs, and ultimately their proper morphogenesis.

## 3. Discussion

In this paper we describe a novel inverted optic vesicle phenotype in $Arl13b^{-/-}$ embryos consequence of defective primary cilia. We argue that this defect is likely a direct consequence of upregulation of *Shh* signaling, that in turn leads to an abnormal increase in cell proliferation in the "ventralized optic vesicles". We also show that the inverted eye phenotype can be rescued by knock-down of Gli2 activity.

How different alterations in primary cilia result in variable types of eye and brain defects is still not known. Although most of those alterations will impact the *Shh* pathway to a different extent, additional players are likely also responsible for the variable phenotypes. It is well known that primary cilia is important during embryogenesis and some mutant mouse models have been characterized (Goetz and Anderson, 2010). However, not much is known about the role of primary cilia in the context of eye development. A recent work about the role of the intra-flagelar transport (IFT) proteins IFT122 and IFT172 suggested that proper assembly of primary cilia is critical for restricting the *Shh* pathway during eye formation in the mouse (Burnett et al., 2017). The authors found that IFT172 mutant embryos lacking primary cilia exhibit modest ectopic *Shh* activity in the distal OV resulting in a proximalized optic cup with expanded RPE and reduced NR. Alternatively, IFT122 mutants with strong ectopic *Shh* signaling have cilia with abnormal morphology (similar to *Arl13b* mutants), and do not form optic cups or lenses, therefore they fail to specify RPE and NR cell types (Burnett et al., 2017). Those different phenotypes between primary cilia mutants could be related to differences in the amount and localization of the ectopic *Shh* signaling, as well as with the defective intercellular signaling components involved in the pathway. Besides the comparative work between IFT122 and IFT172 (Burnett et al., 2017), it was documented that others IFT mutant models such as IFT52, IFT57 and IFT88 have a reduction in *Gli2/Gli3* processing and *Shh* signaling (Gerdes et al., 2009); instead, disruption in *Arl13b* leads

to low levels of constitutively active Gli2 and normal Gli3 repressor activity (Caspary et al., 2007). However, it was recently shown that Arl13 has two different functions depending on the localization of the protein. Arl13b′s role in ciliogenesis is within cilia, whereas its role as a regulator of *Shh* signaling appears to be from outside the cilium (Gigante et al., 2019).

Not all ciliopathy phenotypes can be explained by defective *Shh* signaling (Wallingford and Mitchell, 2011), as demonstrated by Rfx3 mouse mutants with short cilia but apparently unaffected Shh activity (Bonnafe et al., 2004), evidence supporting a direct relationship between primary cilia and abnormal *Shh* signaling (Goetz and Anderson, 2010). It is worth noting that between different cilia mutations affecting the Shh pathway, not all result in loss of Shh signaling, thereby suggesting that the cilium provides more than just a permissive context for Shh signaling, (reviewed in (Bangs and Anderson, 2017). *Shh* deletion leads to the dorsalization of the ventral telencephalon (Chiang et al., 1996), while its overactivation results in the dorsal expansion of ventral-specific genes including Nkx2.1 (Goodrich et al., 1997). Partial recovery of the inverted eye phenotype in $Arl13b^{-/-};Gli2^{Lacz/+}$ double mutant embryos suggests that this phenotype is affecting a *Shh*-dependent pathway. The extent of the rescued phenotype is variable, likely consequence of incomplete penetrance, thereby suggesting that other factors besides Gli2 (Shh pathway) may interact with Arl13b to regulate eye development. It has been demonstrated that ectopic expression of Shh in the optic vesicles could abolish the expression of Bmp4 in the retina (Zhang and Yang, 2001). One of the effectors proteins involved in Bmp4 signaling in the optic vesicles is Lhx2 (Yun et al., 2009). Interestingly $Lhx2^{-/-}$ mice develop optic vesicles but the morphogenetic process is arrested such that optic cup and lens formation fails (Porter et al., 1997; Yun et al., 2009). Conditional deletion of *Lhx2* at different developmental stages showed that the degree of progress in optic vesicle development is critically dependent on the stage at which *Lhx2* activity is removed (Roy et al., 2013) leading to the proposal that *Lhx2* is not essential for eye field specification (Hagglund et al., 2011). We showed that Lhx2 expression is severely reduced in E9.5 mutant optic vesicles (Fig. 3 C, C'); however, its expression in these tissues appears to be restored at around E12.5 (data not shown). Furthermore, expression of the dorsal marker Tbx5 was missing in the mutant optic cups supporting the idea that the ectopic dorsal expression of Shh is affecting the patterning of the optic vesicles.

Excessive *Shh* signaling also promotes Pax2 expression at the expense of Pax6 suppression (Ekker et al., 1995; Macdonald et al., 1995; Perron et al., 2003). This is well documented in the case of mutant embryos lacking the *Shh* antagonist Fkbp8 (Bulgakov et al., 2004) during CNS development. In these mutant embryos, eyes are smaller and have a thinner neuroretina layer, exhibit a hypo-pigmented pigment epithelium and lens morphogenesis is delayed; most defects are associated with an ectopic and ligand-independent activation of the *Shh* pathway. In these embryos Pax2 is expressed ectopically in the dorsal optic vesicles, Pax6 expression is reduced in the neural retina, and the optic cup is internalized into the cephalic mesenchyme (Bulgakov et al., 2004). Interestingly, consistent with inappropriate activation of the *Shh* pathway, we also identified some of those same molecular alterations in $Arl13b^{-/-}$ mutant embryos. In $Arl13b^{-/-}$ embryos the expression pattern of Pax2 and some of the eye phenotypes are similar to the ones reported for $Fkbp8^{-/-}$ embryos (Bulgakov et al., 2004). However, different to $Fkbp8^{-/-}$ embryos, the neuroretina and RPE in $Arl13b^{-/-}$ mice appeared normal (Fig. 1C', D'), and their inverted OVs phenotype seems rather unique.

It was previously reported that Gli activators can regulate Nkx2.1 (Gulacsi and Anderson, 2008), and that Nkx2-1 expression is reduced in *Gli2* knock-out mice. Furthermore, double deletion of Gli1 and Gli2 results in a more severe phenotype such that Nkx2.1 expression is completely lacking in those mutant embryos (Park et al., 2000). We showed that in *Arl13b*$^{-/-}$ embryos there is an ectopic expansion of Nkx2.1 into the dorsal diencephalon (Fig. 5D, D'). Additionally, numerous G1 cyclins are transcriptional targets of Shh-mediated mitogenic response (Kenney and Rowitch, 2000). Shh is required for cyclinD1 expression and the consequent growth of the diencephalon in mouse embryos (Ishibashi and McMahon, 2002). Therefore, Shh ectopic expression in the dorsal diencephalon could be the link between the patterning alterations and the increase in proliferation observed in the dorsal diencephalon and optic vesicles. This data supports the proposal that ectopic *Shh* signaling activation is likely responsible for the inverted OV phenotype in *Arl13b*$^{-/-}$ embryos.

It is worth commenting about the associated lens phenotype in which the Pdgfrα -positive germinal epithelium and the developing Prox1-positve lens fibers are also inverted in the mutant eye, such that the lens fibers appear to be elongating toward the opposite direction that in normal controls. Although in the *Ar13b*$^{-/-}$ embryos the initial induction of the lens vesicle was unaffected (lens placode was induced as indicated by Six3 and Pax6 expression), we noticed that the lens was inverted and that there was minimal elongation of the lens fibers towards the anterior epithelium. We argue that the aberrant lens phenotype seen in *Arl13b*$^{-/-}$ embryos is likely a secondary consequence of the defective OV patterning and movement that eventually engulfs the lens.

In conclusion, we show that *Shh* signaling is upregulated in *Arl13b*$^{-/-}$ dorsal diencephalon and that it plays a role in ventralizing the mutant OVs (Heavner and Pevny, 2012) leading to a change in the dorso-ventral patterning of the optic vesicles. The scheme included in Fig. 7, as well as the whole mount immunostaining followed by tissue clearing (iDISCO) and 3D reconstruction of acquired images shown in Suppl Fig. 2 and Suppl Videos 1 and 2, summarize the defective morphogenetic process resulting from the loss of *Arl13b*. In WT embryos, the initial step of Rax-expressing OVs evaginating from the ventral diencephalon occurs at E9.5 (Figs. 7A and 1-2). At E10.5, a coordinate invagination process of the lens placode and the OV generate the lens vesicle and the double layered optic cup (Figs. 7B and 3). The inner layer is the NR while the external layer becomes the RPE. The lens vesicle remains between the NR and the ectoderm (Figs. 7C and 4) (Heavner and Pevny, 2012). However, at around E9.5 the Rax-expressing mutant OVs become abnormally elongated and bend toward the ventral portion of the head (Fig. 7A', and 6-7). In the mutant embryos, the surface ectoderm is still capable of interacting with the OVs such that the lens placode and lens vesicles are normally formed; however, the invagination of the lens placode appears abnormal, likely consequence of the change in the morphology and in the dorsal-ventral patterning alterations of the optic vesicles (Fig. 7B' and 7-8). Finally, the lens gets engulfed by the NR and RPE, such that its orientation is inverted and the aperture is facing toward the inside of the diencephalic stalk (Fig. 7C' and 9). This abnormal growth pattern of the OVs causes the ventral NR to completely surround the lens vesicle, thereby generating an inverted eye. It's interesting to note that despite these major alterations in eye morphogenesis, *Arl13b*$^{-/-}$ embryos have eyelids and remnants of the anterior eye chamber (Fig. 7, 10).

# 4. Materials and methods

## 4.1. Mice

***Arl13b***$^{+/-}$ mice were kindly provided by E. Anton (UNC Neuroscience Center) and were previously described (Caspary et al., 2007). Genotyping was performed using specific primers to identify the point mutation.

***Six3***$^{Cre/+}$ mice were previously described (Furuta et al., 2000). Primers spanning the *Cre* and the *Six3* sequences were used for PCR genotyping.

***Wnt1***$^{Cre/+}$ mice were purchased from Jackson Laboratory (Stock No:009107). Primers spanning the *Cre* and the *Wnt1* sequence were used for PCR genotyping.

***Gli2***$^{Lacz/+}$ mice were kindly provided by Alexandra Joyner (Memorial Sloan Kettering) (Bai and Joyner, 2001). Two set of primers were used for PCR genotyping. Primers spanning the *LacZ* and the endogenous *Gli2* sequences and primers to detect WT *Gli2* allele were used.

***Arl13b***$^{loxP/loxP}$ mice were kindly provided by S. Zakharenko (St. Jude Children's Research Hospital) (Su et al., 2012). PCR genotyping uses primers that distinguish the wild type and floxed *Arl13b* alleles.

Embryonic stages were assessed from the day of the vaginal plug that was designated as E0.5. All experimental procedures involving animals in this study were approved by IACUC and Northwestern University.

## 4.2. Immunohistochemistry

Standard protocols for embryos (Liu et al., 2006; Takata et al., 2017) were used. Briefly, embryos for immunohistochemistry were dissected in PBS and fixed in 4% paraformaldehyde in 0.1 M PBS (pH 7.4). After overnight protection in 30% sucrose/PBS, tissues were embedded in sucrose:OCT (Tissue-Tek) and sectioned in a cryostat. The following antibodies were used: anti-Arl13b (1:50; NeuroMab clone N295B/66), anti-Acetylated tubulin (1:1000, Sigma, T6793), anti-Rax (1:1000; TaKaRa, M229), anti-Six3 (1:1000; Rockland, custom), anti-Pax6 (1:250; Covance, PRB-278P), anti-Otx2 (1:1000, R&D systems, AF1979-SP), anti-Ki67 (1:200, Invitrogen, MA5-14520), anti-Mitf (1:1000; provided by H. Arnheiter, National Institute of Neurological Disorders and Stroke), anti-Vsx2 (1:500; Exalpha, x1179P and x1180P), anti-β-Crystallin (1:1000; provided by J.S. Zigler, Wilmer Eye Institute, Johns Hopkins Hospital, Baltimore, Maryland), anti-Prox1 (1:500, AngioBio, #11002), anti-Laminin (LAMA1, 1:250, Sigma, L9393), anti-Shh (1:100 DSHB, 5E1), anti-Lhx2 (1:50, Santa Cruz, Sc19342), anti-PdgfRα (1:100, R&D systems, AF1062), anti-Nkx2.1(1:100, Cell signal D2E8), anti-Vax2 (1:100; provided by G. Lemke, Salk Institute for Biological Studies, La Jolla, California), anti-Pax2 (1:50, Biologend, 901001), anti-Tbx5 (1:100, Santa Cruz, SC-515536). anti-Sox1 (1:250, CST #4194). The secondary antibodies were Alexa-488, Cy3, and Cy5 (1:200; Molecular Probes and Jackson Immuno Research), DAPI (1:1000) for DNA and Alexa Fluor® 647 Phalloidin (Thermo fisher, A22287) for F-Actin. Images were obtained with a Zeiss Axioscope.

### 4.3. Whole mount in situ hybridization

It was performed as described (O. V. Lagutin et al., 2003; Takata et al., 2017). *Shh* in situ probe was a gift from Andrew McMahon and *Gli1* in situ probe a gift from Alexandra Joyner.

### 4.4. Whole tissue clearing, 3D imaging and reconstruction

Whole-mount immunostained tissues were tissue cleared according to an iDISCO protocol (kindly provided by Dr. Kristy Red-Horse). Primary antibody was used as follows: Rax (guinea pig, 1/500, TaKaRa). Cy3 (Jackson) was used as dye conjugated to secondary antibodies. Z-stack images were acquired by an inverted microscope equipped with a spinning disk confocal system. The image analysis was initially done by ImageJ analysis. Briefly, the divide function was used in ImageJ image calculator to reduce autofluorescence background signals using signals from the far-red channel. These images were subsequently used to reconstruct three-dimensional images using Imaris software. The movies were generated with the motion function in the Imaris.

### 4.5. Cell counting

We quantified the number of proliferating and apoptotic cells by staining for Ki67 and TUNEL and normalizing the total number of cells in the optic vesicles using ImageJ software (version 2.0.0-rc-69/1.52i). To define the area for quantification we used anatomical features to define the optic vesicle. Cells were counted in two optic vesicle sections from five *Arl13b*$^{+/-}$ and *Arl13b*$^{-/-}$ embryos (all sections are at the same level at the connection between the optic vesicle with the ventral diencephalon).

### 4.6. Statistics

All experiments were performed from a minimum of 3 independent experiments. Values are expressed as mean ± S.E.M (standard error of the mean). Results were analyzed using GraphPad Prism, using student t-test (GraphPad Software). Differences with $P < 0.05$ were considered statistically significant.

## Supplementary Material

Refer to Web version on PubMed Central for supplementary material.

## Acknowledgments

We are grateful to the members of Dr. Beatriz Sosa-Pineda and Dr. Guillermo Oliver laboratories for helpful discussions. LF thanks David Tentler (Northwestern University, Department of Physiology) for comments. Imaging work was performed at the Northwestern University Center for Advanced Microscopy that is generously supported by NCI CCSG P30 CA060553 awarded to the Robert H Lurie Comprehensive Cancer Center.

## References

Adler R, Canto-Soler MV, 2007. Molecular mechanisms of optic vesicle development: complexities, ambiguities and controversies. Dev. Biol 305 (1), 1–13. 10.1016/j.ydbio.2007.01.045. [PubMed: 17335797]

Ashery-Padan R, Marquardt T, Zhou X, Gruss P, 2000. Pax6 activity in the lens primordium is required for lens formation and for correct placement of a single retina in the eye. Genes Dev. 14 (21), 2701–2711. 10.1101/gad.184000. [PubMed: 11069887]

Bai CB, Joyner AL, 2001. Gli1 can rescue the in vivo function of gli2. Development 128 (24), 5161–5172. [PubMed: 11748151]

Bangs F, Anderson KV, 2017. Primary cilia and mammalian hedgehog signaling. Cold Spring Harb. Perspect. Biol 9 (5) 10.1101/cshperspect.a028175.

Barbieri AM, Broccoli V, Bovolenta P, Alfano G, Marchitiello A, Mocchetti C, Banfi S, 2002. Vax2 inactivation in mouse determines alteration of the eye dorsal-ventral axis, misrouting of the optic fibres and eye coloboma. Development 129 (3), 805–813. [PubMed: 11830579]

Belanger MC, Robert B, Cayouette M, 2017. Msx1-positive progenitors in the retinal ciliary margin give rise to both neural and non-neural progenies in mammals. Dev. Cell 40 (2), 137–150. 10.1016/j.devcel.2016.11.020. [PubMed: 28011038]

Belgacem YH, Hamilton AM, Shim S, Spencer KA, Borodinsky LN, 2016. The many hats of sonic hedgehog signaling in nervous system development and disease. J. Dev. Biol 4 (4) 10.3390/jdb4040035.

Berbari NF, O'Connor AK, Haycraft CJ, Yoder BK, 2009. The primary cilium as a complex signaling center. Curr. Biol 19 (13), R526–R535. 10.1016/j.cub.2009.05.025. [PubMed: 19602418]

Bharti K, Nguyen MT, Skuntz S, Bertuzzi S, Arnheiter H, 2006. The other pigment cell: specification and development of the pigmented epithelium of the vertebrate eye. Pigm. Cell Res 19 (5), 380–394. 10.1111/j.1600-0749.2006.00318.x.

Bonnafe E, Touka M, AitLounis A, Baas D, Barras E, Ucla C, et al., 2004. The transcription factor rfx3 directs nodal cilium development and left-right asymmetry specification. Mol. Cell Biol 24 (10), 4417–4427. 10.1128/mcb.24.10.4417-4427.2004. [PubMed: 15121860]

Bulgakov OV, Eggenschwiler JT, Hong DH, Anderson KV, Li T, 2004. Fkbp8 is a negative regulator of mouse sonic hedgehog signaling in neural tissues. Development 131 (9), 2149–2159. 10.1242/dev.01122. [PubMed: 15105374]

Burnett JB, Lupu FI, Eggenschwiler JT, 2017. Proper ciliary assembly is critical for restricting hedgehog signaling during early eye development in mice. Dev. Biol 430 (1), 32–40. 10.1016/j.ydbio.2017.07.012. [PubMed: 28778798]

Cantagrel V, Silhavy JL, Bielas SL, Swistun D, Marsh SE, Bertrand JY, Gleeson JG, 2008. Mutations in the cilia gene arl13b lead to the classical form of joubert syndrome. Am. J. Hum. Genet 83 (2), 170–179. 10.1016/j.ajhg.2008.06.023. [PubMed: 18674751]

Caspary T, Larkins CE, Anderson KV, 2007. The graded response to sonic hedgehog depends on cilia architecture. Dev. Cell 12 (5), 767–778. 10.1016/j.devcel.2007.03.004. [PubMed: 17488627]

Chiang C, Litingtung Y, Lee E, Young KE, Corden JL, Westphal H, Beachy PA, 1996. Cyclopia and defective axial patterning in mice lacking sonic hedgehog gene function. Nature 383 (6599), 407–413. 10.1038/383407a0. [PubMed: 8837770]

Chow RL, Lang RA, 2001. Early eye development in vertebrates. Annu. Rev. Cell Dev. Biol 17, 255–296. 10.1146/annurev.cellbio.17.1.255. [PubMed: 11687490]

D'Angelo A, Franco B, 2009. The dynamic cilium in human diseases. Pathogenetics 2 (1), 3. 10.1186/1755-8417-2-3. [PubMed: 19439065]

Dilan TL, Moye AR, Salido EM, Saravanan T, Kolandaivelu S, Goldberg AFX, Ramamurthy V, 2019. Arl13b, a joubert syndrome-associated protein, is critical for retinogenesis and elaboration of mouse photoreceptor outer segments. J. Neurosci 39 (8), 1347–1364. 10.1523/jneurosci.1761-18.2018. [PubMed: 30573647]

Ekker SC, Ungar AR, Greenstein P, von Kessler DP, Porter JA, Moon RT, Beachy PA, 1995. Patterning activities of vertebrate hedgehog proteins in the developing eye and brain. Curr. Biol 5 (8), 944–955. [PubMed: 7583153]

Endoh-Yamagami S, Evangelista M, Wilson D, Wen X, Theunissen JW, Phamluong K, et al., 2009. The mammalian cos2 homolog kif7 plays an essential role in modulating hh signal transduction during development. Curr. Biol 19 (15), 1320–1326. 10.1016/j.cub.2009.06.046. [PubMed: 19592253]

Furuta Y, Lagutin O, Hogan BL, Oliver GC, 2000. Retina- and ventral forebrain-specific cre recombinase activity in transgenic mice. Genesis 26 (2), 130–132. [PubMed: 10686607]

Gerdes JM, Davis EE, Katsanis N, 2009. The vertebrate primary cilium in development, homeostasis, and disease. Cell 137 (1), 32–45. 10.1016/j.cell.2009.03.023. [PubMed: 19345185]

Gigante ED, Taylor MR, Ivanova AA, Kahn RA, Caspary T, 2019. Arl13b Regulates Sonic Hedgehog Signaling from outside Primary Cilia, p. 711671. 10.1101/711671 bioRxiv.

Goetz SC, Anderson KV, 2010. The primary cilium: a signalling centre during vertebrate development. Nat. Rev. Genet 11 (5), 331–344. 10.1038/nrg2774. [PubMed: 20395968]

Goodrich LV, Milenkovic L, Higgins KM, Scott MP, 1997. Altered neural cell fates and medulloblastoma in mouse patched mutants. Science 277 (5329), 1109–1113. [PubMed: 9262482]

Gulacsi AA, Anderson SA, 2008. Beta-catenin-mediated wnt signaling regulates neurogenesis in the ventral telencephalon. Nat. Neurosci 11 (12), 1383–1391. 10.1038/nn.2226. [PubMed: 18997789]

Hagglund AC, Dahl L, Carlsson L, 2011. Lhx2 is required for patterning and expansion of a distinct progenitor cell population committed to eye development. PloS One 6 (8), e23387. 10.1371/journal.pone.0023387. [PubMed: 21886788]

Heavner W, Pevny L, 2012. Eye development and retinogenesis. Cold Spring Harb. Perspect. Biol 4 (12) 10.1101/cshperspect.a008391.

Horner VL, Caspary T, 2011. Disrupted dorsal neural tube bmp signaling in the cilia mutant arl13b hnn stems from abnormal shh signaling. Dev. Biol 355 (1), 43–54. 10.1016/j.ydbio.2011.04.019. [PubMed: 21539826]

Houde C, Dickinson RJ, Houtzager VM, Cullum R, Montpetit R, Metzler M, et al., 2006. Hippi is essential for node cilia assembly and sonic hedgehog signaling. Dev. Biol 300 (2), 523–533. 10.1016/j.ydbio.2006.09.001. [PubMed: 17027958]

Huangfu D, Anderson KV, 2005. Cilia and hedgehog responsiveness in the mouse. Proc. Natl. Acad. Sci. U. S. A 102 (32), 11325–11330. 10.1073/pnas.0505328102. [PubMed: 16061793]

Huangfu D, Liu A, Rakeman AS, Murcia NS, Niswander L, Anderson KV, 2003. Hedgehog signalling in the mouse requires intraflagellar transport proteins. Nature 426 (6962), 83–87. 10.1038/nature02061. [PubMed: 14603322]

Ishibashi M, McMahon AP, 2002. A sonic hedgehog-dependent signaling relay regulates growth of diencephalic and mesencephalic primordia in the early mouse embryo. Development 129 (20), 4807–4819. [PubMed: 12361972]

Kenney AM, Rowitch DH, 2000. Sonic hedgehog promotes g(1) cyclin expression and sustained cell cycle progression in mammalian neuronal precursors. Mol. Cell Biol 20 (23), 9055–9067. [PubMed: 11074003]

Lagutin O, Zhu CC, Furuta Y, Rowitch DH, McMahon AP, Oliver G, 2001. Six3 promotes the formation of ectopic optic vesicle-like structures in mouse embryos. Dev. Dynam 221 (3), 342–349. 10.1002/dvdy.1148.

Lagutin OV, Zhu CC, Kobayashi D, Topczewski J, Shimamura K, Puelles L, Oliver G, 2003. Six3 repression of wnt signaling in the anterior neuroectoderm is essential for vertebrate forebrain development. Genes Dev. 17 (3), 368–379. 10.1101/gad.1059403. [PubMed: 12569128]

Larkins CE, Aviles GD, East MP, Kahn RA, Caspary T, 2011. Arl13b regulates ciliogenesis and the dynamic localization of shh signaling proteins. Mol. Biol. Cell 22 (23), 4694–4703. 10.1091/mbc.E10-12-0994. [PubMed: 21976698]

Lebel M, Mo R, Shimamura K, Hui CC, 2007. Gli2 and gli3 play distinct roles in the dorsoventral patterning of the mouse hindbrain. Dev. Biol 302 (1), 345–355. 10.1016/j.ydbio.2006.08.005. [PubMed: 17026983]

Liu W, Lagutin O, Swindell E, Jamrich M, Oliver G, 2010. Neuroretina specification in mouse embryos requires six3-mediated suppression of wnt8b in the anterior neural plate. J. Clin. Invest. 120 (10), 3568–3577. 10.1172/jci43219. [PubMed: 20890044]

Liu W, Lagutin OV, Mende M, Streit A, Oliver G, 2006. Six3 activation of pax6 expression is essential for mammalian lens induction and specification. EMBO J. 25 (22), 5383–5395. 10.1038/sj.emboj.7601398. [PubMed: 17066077]

Macdonald R, Barth KA, Xu Q, Holder N, Mikkola I, Wilson SW, 1995. Midline signalling is required for pax gene regulation and patterning of the eyes. Development 121 (10), 3267–3278. [PubMed: 7588061]

Makino S, Tampo H, 2014. Ocular findings in two siblings with joubert syndrome. Clin. Ophthalmol 8, 229–233. 10.2147/opth.S58672. [PubMed: 24531165]

Malone AM, Anderson CT, Tummala P, Kwon RY, Johnston TR, Stearns T, Jacobs CR, 2007. Primary cilia mediate mechanosensing in bone cells by a calcium-independent mechanism. Proc. Natl. Acad. Sci. U. S. A 104 (33), 13325–13330. 10.1073/pnas.0700636104. [PubMed: 17673554]

Martinez-Morales JR, Rodrigo I, Bovolenta P, 2004. Eye development: a view from the retina pigmented epithelium. Bioessays 26 (7), 766–777. 10.1002/bies.20064. [PubMed: 15221858]

Mo R, Freer AM, Zinyk DL, Crackower MA, Michaud J, Heng HH, et al., 1997. Specific and redundant functions of gli2 and gli3 zinc finger genes in skeletal patterning and development. Development 124 (1), 113–123. [PubMed: 9006072]

Mui SH, Kim JW, Lemke G, Bertuzzi S, 2005. Vax genes ventralize the embryonic eye. Genes Dev. 19 (10), 1249–1259. 10.1101/gad.1276605. [PubMed: 15905411]

Nishimura Y, Kasahara K, Shiromizu T, Watanabe M, Inagaki M, 2019. Primary cilia as signaling hubs in health and disease. Adv. Sci. 6 (1), 1801138. 10.1002/advs.201801138.

Oliver G, Mailhos A, Wehr R, Copeland NG, Jenkins NA, Gruss P, 1995. Six3, a murine homologue of the sine oculis gene, demarcates the most anterior border of the developing neural plate and is expressed during eye development. Development 121 (12), 4045–4055. [PubMed: 8575305]

Park HL, Bai C, Platt KA, Matise MP, Beeghly A, Hui CC, et al., 2000. Mouse gli1 mutants are viable but have defects in shh signaling in combination with a gli2 mutation. Development 127 (8), 1593–1605. [PubMed: 10725236]

Perron M, Boy S, Amato MA, Viczian A, Koebernick K, Pieler T, Harris WA, 2003. A novel function for hedgehog signalling in retinal pigment epithelium differentiation. Development 130 (8), 1565–1577. [PubMed: 12620982]

Porter FD, Drago J, Xu Y, Cheema SS, Wassif C, Huang SP, et al., 1997. Lhx2, a lim homeobox gene, is required for eye, forebrain, and definitive erythrocyte development. Development 124 (15), 2935–2944. [PubMed: 9247336]

Rowitch DH, B SJ, Lee SM, Flax JD, Snyder EY, McMahon AP, 1999. Sonic hedgehog regulates proliferation and inhibits differentiation of cns precursor cells. J. Neurosci 19 (20), 8954–8965. [PubMed: 10516314]

Roy A, de Melo J, Chaturvedi D, Thein T, Cabrera-Socorro A, Houart C, et al., 2013. Lhx2 is necessary for the maintenance of optic identity and for the progression of optic morphogenesis. J. Neurosci 33 (16), 6877–6884. 10.1523/jneurosci.4216-12.2013. [PubMed: 23595746]

Su CY, Bay SN, Mariani LE, Hillman MJ, Caspary T, 2012. Temporal deletion of arl13b reveals that a mispatterned neural tube corrects cell fate over time. Development 139 (21), 4062–4071. 10.1242/dev.082321. [PubMed: 23014696]

Takata N, Abbey D, Fiore L, Acosta S, Feng R, Gil HJ, et al., 2017. An eye organoid approach identifies six3 suppression of r-spondin 2 as a critical step in mouse neuroretina differentiation. Cell Rep. 21 (6), 1534–1549. 10.1016/j.celrep.2017.10.041. [PubMed: 29117559]

Take-uchi M, Clarke JD, Wilson SW, 2003. Hedgehog signalling maintains the optic stalk-retinal interface through the regulation of vax gene activity. Development 130 (5), 955–968. [PubMed: 12538521]

Thomas S, Wright KJ, Le Corre S, Micalizzi A, Romani M, Abhyankar A, et al., 2014. A homozygous pde6d mutation in joubert syndrome impairs targeting of farnesylated inpp5e protein to the primary cilium. Hum. Mutat 35 (1), 137–146. 10.1002/humu.22470. [PubMed: 24166846]

Valente EM, Brancati F, Dallapiccola B, 2008. Genotypes and phenotypes of joubert syndrome and related disorders. Eur. J. Med. Genet 51 (1), 1–23. 10.1016/j.ejmg.2007.11.003. [PubMed: 18164675]

Valente EM, Dallapiccola B, Bertini E, 2013. Joubert syndrome and related disorders. Handb. Clin. Neurol 113, 1879–1888. 10.1016/b978-0-444-59565-2.00058-7. [PubMed: 23622411]

Vierkotten J, Dildrop R, Peters T, Wang B, Ruther U, 2007. Ftm is a novel basal body protein of cilia involved in shh signalling. Development 134 (14), 2569–2577. 10.1242/dev.003715. [PubMed: 17553904]

Wallingford JB, Mitchell B, 2011. Strange as it may seem: the many links between wnt signaling, planar cell polarity, and cilia. Genes Dev. 25 (3), 201–213. 10.1101/gad.2008011. [PubMed: 21289065]

Ware SM, Aygun MG, Hildebrandt F, 2011. Spectrum of clinical diseases caused by disorders of primary cilia. Proc. Am. Thorac. Soc 8 (5), 444–450. 10.1513/pats.201103-025SD. [PubMed: 21926397]

Wheway G, Parry DA, Johnson CA, 2014. The role of primary cilia in the development and disease of the retina. Organogenesis 10 (1), 69–85. 10.4161/org.26710. [PubMed: 24162842]

Wood HB, Episkopou V, 1999. Comparative expression of the mouse sox1, sox2 and sox3 genes from pre-gastrulation to early somite stages. Mech. Dev 86 (1–2), 197–201. [PubMed: 10446282]

Yun S, Saijoh Y, Hirokawa KE, Kopinke D, Murtaugh LC, Monuki ES, Levine EM, 2009. Lhx2 links the intrinsic and extrinsic factors that control optic cup formation. Development 136 (23), 3895–3906. 10.1242/dev.041202. [PubMed: 19906857]

Zhang XM, Yang XJ, 2001. Temporal and spatial effects of sonic hedgehog signaling in chick eye morphogenesis. Dev. Biol 233 (2), 271–290. 10.1006/dbio.2000.0195. [PubMed: 11336495]

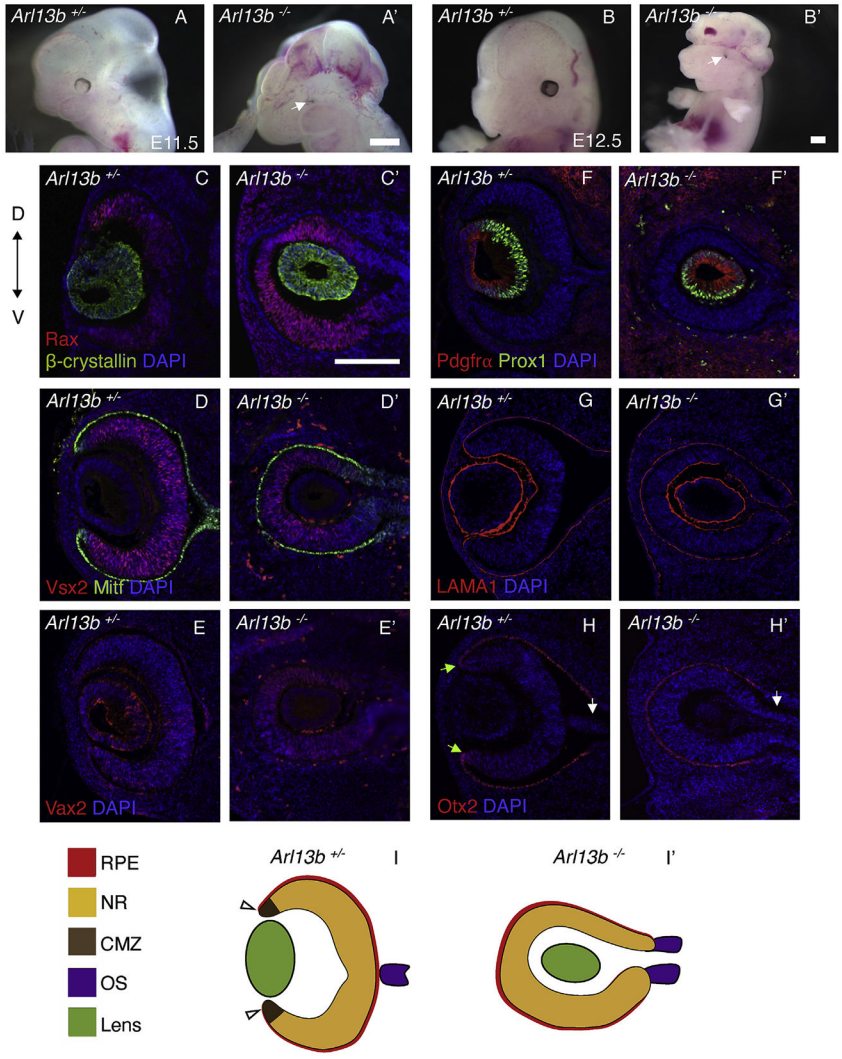


**Fig. 1. Optic cups are inverted in *Arl13b*$^{-/-}$ embryos.**

At E11.5, eye defects are obvious in *Arl13b*$^{-/-}$ embryos (**A′**). Defects are also seen at E12.5 (**B′**). White arrows indicate the defective eyes. Immunostaining against Rax and β-crystallin shows the normal optic cup and lens in *Arl13b*$^{+/-}$ embryos (**C**). However, in *Arl13b*$^{-/-}$ littermates (**C′**) the opening of the optic cup is inverted. Immunostaining against Mitf and Vsx2 shows that the RPE is abnormally facing the surface ectoderm in *Arl13b*$^{-/-}$ embryos and the NR is entirely surrounded by the RPE (**D′**). Vax2 is ectopically expressed all around the mutant NR (**E′**) instead, its expression is localized in the ventral NR in *Arl13b*$^{+/-}$ littermates (**E**). Prox1 and Pdgfrα staining of the lens fibers and lens germinal epithelium shows that the lens is inverted in the mutant embryos (**F′**). Laminin is expressed in the basal part of the NR, RPE and lens in *Arl13*$^{+/-}$ (**G**) and *Arl13* $^{-/-}$ (**G′**) embryos. Immunostaining against Otx2 in *Arl13b*$^{+/-}$ (**H**) and *Arl13b* $^{-/-}$ (**H′**) embryos shows the RPE in both embryos, but the CMZ (green arrow) is only detected in control *Arl13b*$^{+/-}$ embryos. White arrows show the optic stalk. Schematic representation of the E12.5 *Arl13b*$^{+/-}$ (**I**) and *Arl13b* $^{-/-}$ (**I′**) eyes. Scale bar: 100 μm. (N: 3).

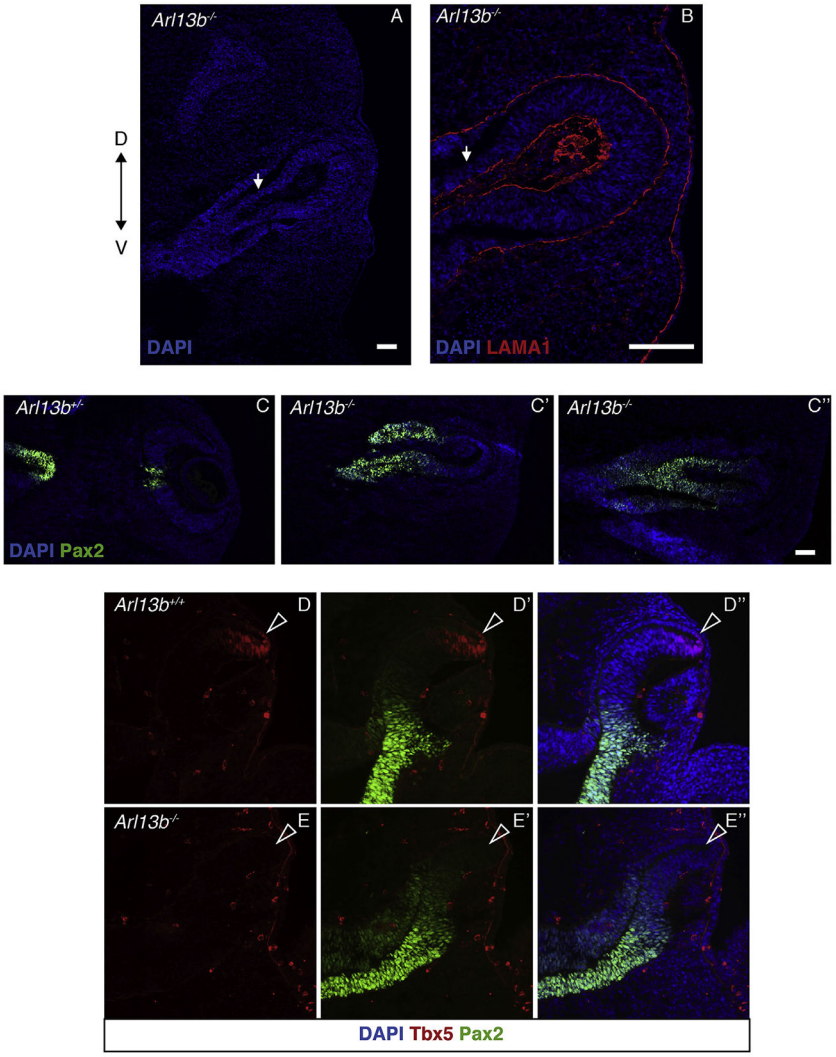


**Fig. 2. The optic stalk is defective in *Arl13*$^{-/-}$ embryos.**

Immunostaining against laminin (LAMA1) indicates the basal polarity of the optic stalk in *Arl13b*$^{-/-}$ embryos **(B),** white arrow indicates the optic stalk. In *Arl13b*$^{+/-}$ embryos, Pax2 is expressed in the central retina and optic stalk **(C),** instead, in *Arl13b*$^{-/-}$ embryos in addition to the optic stalk, Pax2 is also ectopically expressed in the proximal segment of the inner layer of the optic cup (**C′, C″**). Immunohistochemistry against Tbx5 and Pax2 in E10.5 *Arl13b*$^{+/-}$ (**D-D″**) and *Arl13b* $^{-/-}$ (**E-E″**) optic cups. In the mutant embryos Pax2 expression is dorsally expanded and that of Tbx5 is missing (white arrowheads indicate the putative dorsal eye territory). Scale bar: 100 μm. (N: 3).

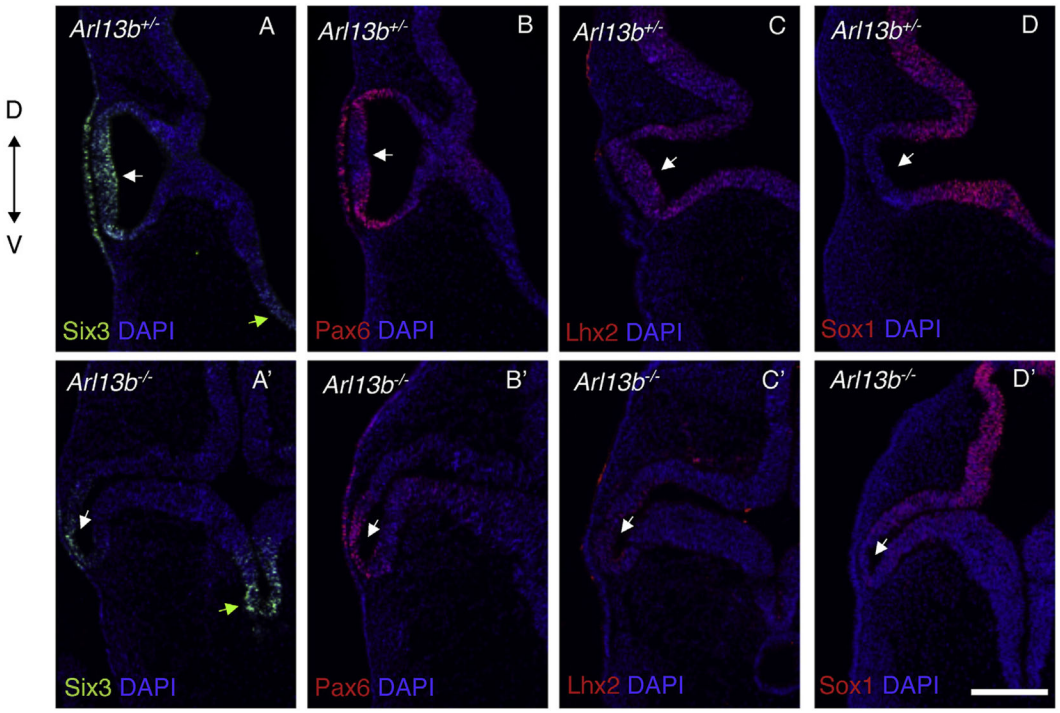


**Fig. 3. Optic vesicles are defective in *Arl13b*$^{-/-}$.**

Immunostaining against Six3 (**A, A′**), Pax6 (**B, B′**), Lhx2 (**C, C′**) and Sox1 (**D, D′**) in E9.5 embryos. Six3 and Pax6 are classical eye markers whose expression is still detected in the *Arl13b*$^{-/-}$ OVs and lens placode **(A′-B′)** although at a lower levels and extension in comparison with *Arl13b*$^{+/-}$ littermates (**A-B**). Lhx2 expression is dramatically reduced in the mutant optic vesicles (**C′**). Sox1, a gene that is not normally expressed in the OVs (**D**), is abnormally detected in this tissue in the *Arl13b*$^{-/-}$ OVs (**D′**). Those results indicate that at E9.5 patterning is affected in *Arl13b* $^{-/-}$ embryos with the OVs abnormally bending toward the ventral diencephalon. Green arrows indicate the ventral diencephalon (**A, A′**). White arrows indicate OVs (**A- D′**). Scale bar: 100 μm. (N: 3).

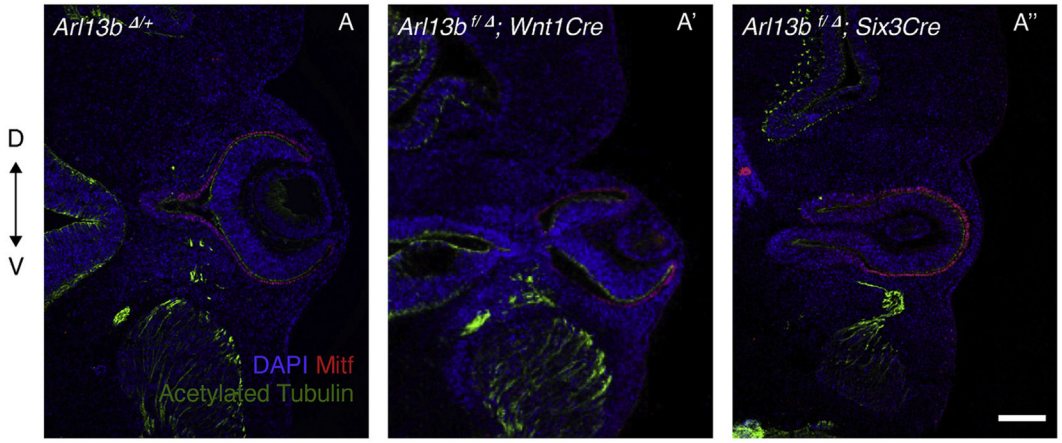


**Fig. 4. Arl13b activity in the forebrain is necessary for proper OV morphogenesis.**

OV morphogenesis appears normal upon conditional deletion of *Arl13b* using $Wnt1^{Cre}$ at E11.5 (**A′**). Conditional deletion using $Six3^{Cre}$ recapitulates the same inverted optic cup phenotype seen in $Arl13b^{-/-}$ embryos. Immunostaining is against Mitf (RPE marker) and acetylated tubulin (primary cilia and axon marker). Scale bar: 100 μm. (N: 3).

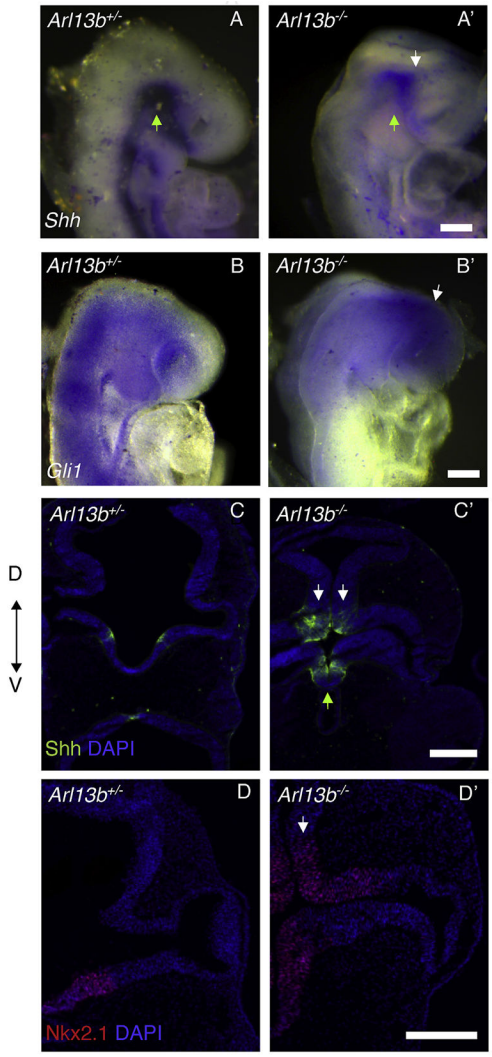


**Fig. 5. Loss of *Arl13b* affects *Shh* signaling.**

E9.5 whole-mount in situ hybridization against *Shh* in *Arl13b* $^{+/-}$ (**A**) and *Arl13b*$^{-/-}$ (**A′**) embryos shows reduced expression in the ventral diencephalon (green arrow) and ectopic expression in the dorsal side (white arrow) of the mutant embryos. As expected, in situ hybridization against *Gli1*, a readout for *Shh* signaling, shows *Gli1* ectopic expression in the dorsal diencephalon (white arrow) and forebrain of *Arl13b*$^{-/-}$ embryos (**B′**). Immunostaining against Shh (**C–C′**) confirms the ectopic expression of Shh in the dorsal diencephalon (white arrow: dorsal diencephalon and green arrow: ventral diencephalon). Immunostaining against the downstream Shh signaling effector Nkx2.1 shows that it is ectopically expressed in the dorsal diencephalon (white arrow) of *Arl13b*$^{-/-}$ (**D-D′**) embryos. Scale bar: 100 μm. (N: 3).

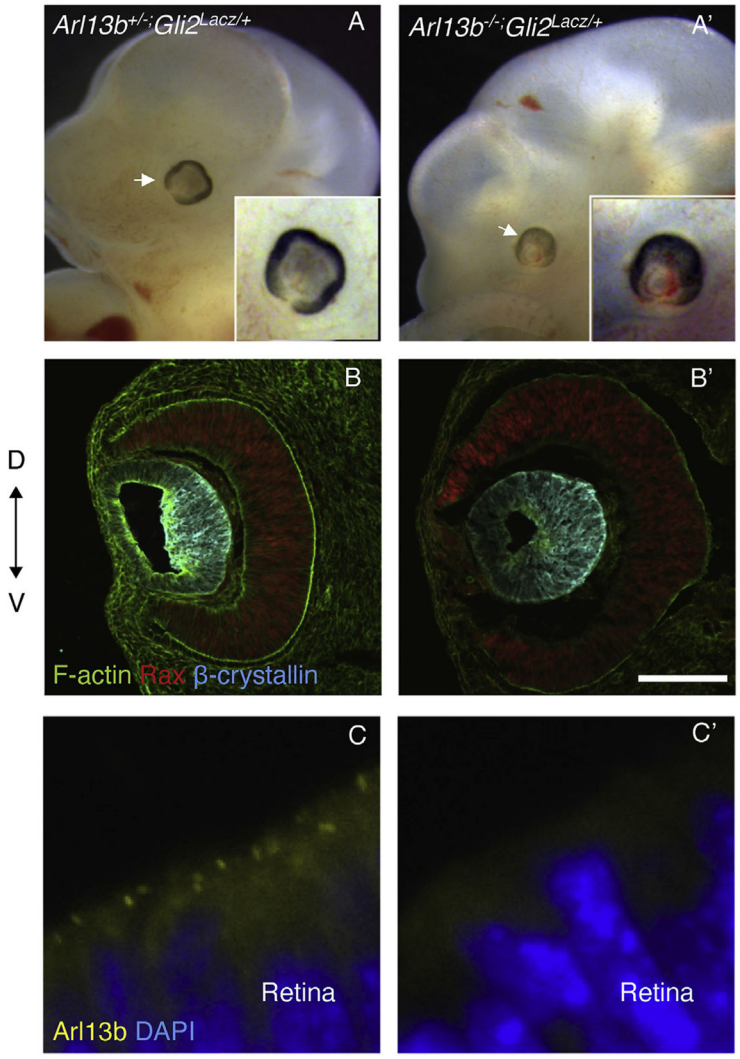


**Fig. 6. The inverted eye phenotype is rescued by removing the *Shh* signaling mediator Gli2.**

**(A, A′)** Optic vesicles are normal in *Arl13*$^{+/-}$;*Gli2*$^{Lacz/+}$ embryos. The eye phenotype and brain exencephaly is partially rescued in *Arl13b*$^{-/-}$;*Gli2*$^{Lacz/+}$ embryos. Arrow indicates the eye. (**B, B′**) Immunostaining against the neural retina marker Rax and the lens markers β-crystallin and F-actin reveals that the orientation of the neural retina and lens in *Arl13b*$^{-/-}$;*Gli2*$^{Lacz/+}$ embryos was rescued. (**C, C′**) Immunostaining against Arl13b in *Arl13b*$^{+/-}$ retinas reveals the cilia in the apical side of the neural retina. However, no signal is detected in Arl13b mutant retinas, confirming that the mutant embryos lack Arl13b protein expression. Scale bar: 100 μm. (N: 3).

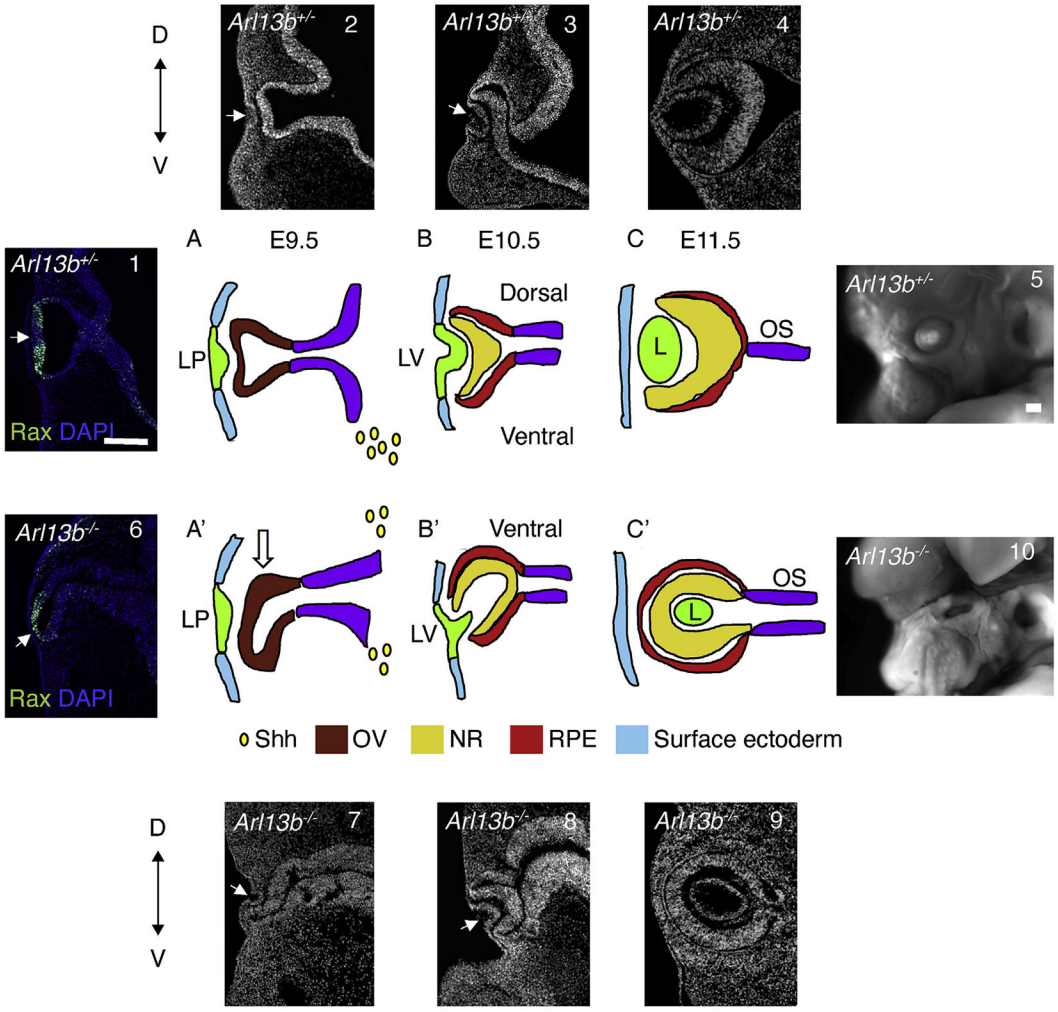


**Fig. 7. Schematic representation of the normal (*Arl13b*$^{+/-}$) and defective (*Arl13b*$^{-/-}$) process of OV morphogenesis.**

Immunostaining against Rax shows the normal shape of the evaginating OV at E9.5 (**1**). (**A, 2**) At around E9.5, in *Arl13b*$^{+/-}$ embryos (WT) the optic vesicles (red) start to evaginate from the adjacent diencephalon (purple) toward the surface ectoderm (E, light blue). Soon after, the distal portion of the OVs contacts the overlying surface ectoderm and induces the formation of the lens placode (light green, LP). This interaction promotes the invagination of the lens placode and of the distal OV resulting in the formation of a bilayered optic cup at around E10.5. *Shh* (yellow drops) from the ventral forebrain is important for proper D-V patterning of the OV. (**B, 3**) At around E10.5, neuroretina (NR, yellow) fate specification will start in the inner layer of the optic cup and the RPE (red) will form in the outer layer. At the same time, the lens vesicle (LV) starts to invaginate. (**C, 4**) By E11.5 the lens (L) separates from the surface ectoderm and differentiates into a mature lens and the most proximal part of the OV narrows to form the optic stalk (purple). (**5**) Image of the normal looking eye in E16.5 embryos. Immunostaining against Rax shows the abnormal shape of the OV at E9.5 (**6**). (**A′**, **7**) In *Arl13*$^{-/-}$ embryos the initial step of optic vesicle evagination appears defective, as the evaginating OV starts to abnormally bend ventrally (arrow). This

alteration is likely consequence of the hyperactivation of *Shh* signal in the dorsal diencephalon that in the mutant embryos appears enlarged and "ventralized". (**B′**, **8**) As the evagination process progresses, the mutant OV keeps moving ventrally engulfing the lens vesicle. (**C′**, **9**) Finally, at around E11.5 the orientation of the optic-vesicle in *Arl13b*$^{-/-}$ embryos is completely inverted, such that the opening is facing toward the inside of the diencephalic stalk instead than to the surface ectoderm. (**10**) Image of the E16.5 mutant eye. LP, lens placode; LV, lens vesicle; L, lens. Scale bar: 100 μm.